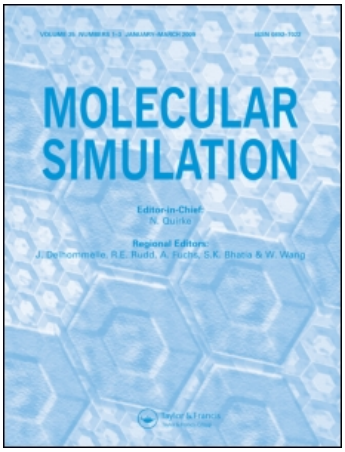

Molecular Simulation
Publication details, including instructions for authors and subscription information:
http://www.informaworld.com/smpp/title~content=t713644482

A Monte Carlo Study of Surface Reconstruction in (100) and (111) Diamond Surfaces and Nanodiamond

A. S. Barnard[a]; P. Bath†[a]; S. P. Russo[a]; I. K. Snook¶[a]
[a] Department of Applied Physics, Royal Melbourne Institute of Technology University, GPO BOXV, Melbourne, Australia

To cite this Article Barnard, A. S. , Bath†, P. , Russo, S. P. and Snook¶, I. K.(2004) 'A Monte Carlo Study of Surface Reconstruction in (100) and (111) Diamond Surfaces and Nanodiamond', Molecular Simulation, 30: 1, 1 — 8
To link to this Article: DOI: 10.1080/08927020310001640061
URL: http://dx.doi.org/10.1080/08927020310001640061

Molecular Simulation, VOL. 30 (1), 15 January 2004, pp. 1–8

Taylor & Francis
Taylor & Francis Group

A Monte Carlo Study of Surface Reconstruction in (100) and (111) Diamond Surfaces and Nanodiamond

A.S. BARNARD*, P. BATH†, S.P. RUSSO‡ and I.K. SNOOK¶

Department of Applied Physics, Royal Melbourne Institute of Technology University, GPO BOX 2476V Melbourne, 3001 Australia

(Received August 2003; In final form September 2003)

A Monte-Carlo (MC) study of the surface reconstruction and relaxation of the diamond (100) and (111) surfaces is presented. Surface reconstruction events have been simulated using as empirical 2 + 3 body potential fitted to *ab initio* data. MC simulations are first performed on thick diamond slabs with (100) and (111) surfaces in order to evaluate the quality of the potential. The results obtained are then compared to those obtained using computational methods and experimental results. Reconstruction results for nanodiamond crystals with (100) surfaces of sizes ranging from 0.5 to 2 nm are then presented and discussed.

Keywords: Monte-Carlo study; Nanodiamond; Diamond slab; Molecular dynamics

INTRODUCTION

Over the past two decades, a variety of empirical and *ab initio* techniques have been applied to simulate the reconstruction of surfaces in diamond lattice semiconductors such as Si, Ge and C [1–8]. Recently, diamond (carbon) based materials have been proposed as the optimal choice for nano-mechanical designs due (mainly) to their high elastic modulus and strength-to-weight ratio. Nanodevices in the size regime of a few to tens of nanometers have been postulated. This size regime corresponds to structures ranging from tens of thousands to a few million atoms. Currently such system sizes can only be computationally studied using empirical Monte-Carlo (MC) or Molecular Dynamics methods.

An important aspect of simulating nanodiamond structures is to correctly model their surfaces. While a great deal of theoretical research has been conduced regarding the reconstruction of diamond surfaces, experimental measurements do not give a complete picture [9] and a complete experimental characterisation has yet to be achieved. Recent studies do show that for bulk diamond and nanodiamond reconstruction occurs via dimerisation for the (100) face [10], while there has been some conjecture as to whether for the (111) surface reconstruction is due to graphitisation or true dimerisation [9,11,12]. It is also unclear if the surfaces favour clean reconstructed (dimerised) surface, or whether hydrogenated (or deuterated) surfaces are energetically favoured [13,14].

We have recently developed a new potential for sp^3 carbon, based on fitting *ab initio* data to a SW potential type functional template, that gives a more accurate prediction of the elastic constants of bulk diamond [15,16] with an aim of using this potential to model nanodiamond structures such as nanorods [17]. As surface reconstruction effects will obviously affect the stability of such systems, which due to their size have a high surface area to volume ratio, we evaluate how our new potential for diamond models surface relaxation and reconstruction for the (100) and (111) surfaces. The relaxed surfaces were calculated using a Metropolis Monte Carlo Algorithm (MC) [18] with our potential.

In this study, only dehydrogenated (clean) diamond surfaces have been considered. Such a study is of intrinsic theoretical interest and also serves as a beginning for a further investigation on

*E-mail: amanda.barnard@physics.org
†E-mail: peter.bath@rmit.edu.au
‡Corresponding author. E-mail: salvy.russo@rmit.edu.au
¶E-mail: ian.snook@rmit.edu.au

ISSN 0892-7022 print/ISSN 1029-0435 online © 2004 Taylor & Francis Ltd
DOI: 10.1080/08927020310001640061

hydrogenated carbon surfaces. The results obtained are then compared to those obtained using empirical potentials, Density Functional Theory (DFT), combined methods; and experimental results. Having evaluated the accuracy of the SW potential in describing surface reconstruction and relaxation, reconstruction results for nanodiamond crystals with (100) surfaces of sizes ranging from 0.5 to 2 nm are presented and discussed.

BACKGROUND

In this study, we used a potential based on fitting to *ab-initio* calculations performed on carbon clusters. The functional template used to fit the data was a Stillinger-Weber type potential, which is a well-known empirical potential for describing tetrahedral bonded covalent semiconductor structures. A detailed description of the potential is given elsewhere [15,19] and we only briefly describe it here. The form of the SW potential is given by:

$$\Phi(r_1) = \sum_{i<j} U^{(2)}(r_{ij}) + \sum_{i\neq j}\sum_{<k} U^{(3)}(r_{ij}, r_{ik}, \theta_{jik}), \quad (1)$$

where

$$U^{(2)} = \begin{cases} \epsilon A\left(\frac{B\sigma^4}{r_{ij}^4} - 1\right)\exp\left\{\frac{\sigma}{(r_{ij}-a\sigma)}\right\} & r_{ij} < a\sigma \\ 0 & r_{ij} \geq a\sigma \end{cases}, \quad (2)$$

$$U^{(3)} = \begin{cases} \epsilon\lambda \exp\left\{\frac{\gamma\sigma}{(r_{ij}-a\sigma)}\right\}\exp\left\{\frac{\gamma\sigma}{(r_{ik}-a\sigma)}\right\} & \\ \qquad \times \left(\cos\theta_{jik} + \frac{1}{3}\right)^2 & r_{ij} < a\sigma, \\ 0 & r_{ij} \geq a\sigma \end{cases} \quad (3)$$

In the above equations $U^{(2)}$ describes bond stretching, $U^{(3)}$ bond bending, while ϵ and σ are the energy and length scaling parameters. The SW two-body term given in equation (2) models the bond stretching of the ij bond. The interaction cutoff $a\sigma$ insures the potential is short ranged. Equation (3) shows the form of the bond bending contribution to the SW potential. θ_{jik} is the angle formed by the ij and ik bond and $U^{(3)}$ is zero when θ_{jik} corresponds to a tetrahedral angle, which ensures that the diamond lattice structure is the minimum energy configuration. The parameters A, B, λ, a, ϵ and σ are fitting parameters which were determined by fitting to *ab-initio* data. The values of the fitted parameters for diamond carbon were [15]:

$$A = 5.3789794, \quad B = 0.5933864, \quad a = 1.846285,$$
$$\sigma = 1.368\,\text{Å}, \quad \epsilon = 3.551\,\text{eV},$$
$$\lambda = 26.19934, \quad \gamma = 1.055116.$$

The Monte Carlo simulations in the study were performed using Metropolis Monte Carlo Algorithm. The MC runs on the (100) and (111) diamond surface were performed for 200 million moves, while for the nanodiamond clusters results were tabulated after 100 million moves. All calculations were performed at 300 K.

RESULTS AND DISCUSSION

In this study, we used a freshly cleaved surface as our initial structure in order to determine the extent of spontaneous reconstruction and relaxation from the bulk. As stated earlier in this study only dehydrogenated (clean) diamond surfaces have been considered. In this study the value 3.56683 Å was used as lattice constant of bulk diamond at 300 K. Previous studies by others [14,20] and our MC simulations have concluded that no true reconstruction is observed on the (110) surface, with only a relaxation involving the straightening of the surface chains occurring. Hence the (110) surface is considered to be reasonable stable. However, a variety of dimer patterns have been observed on the reactive (100) and (111) surface. The features of the reconstructed clean (100) surface addressed here include the (2 × 1) dimer length d_{11}, the secondary (2 × 1) dimer bond d_{12} (see Fig. 1) and the first and second

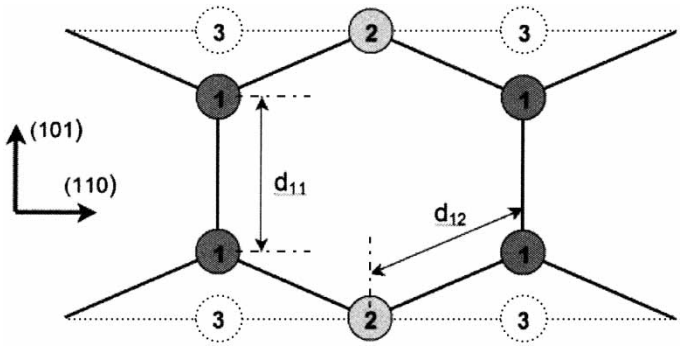

FIGURE 1 Schematic diagram of the d_{11} and d_{12} dimer lengths on the (100) (2 × 1) surface.

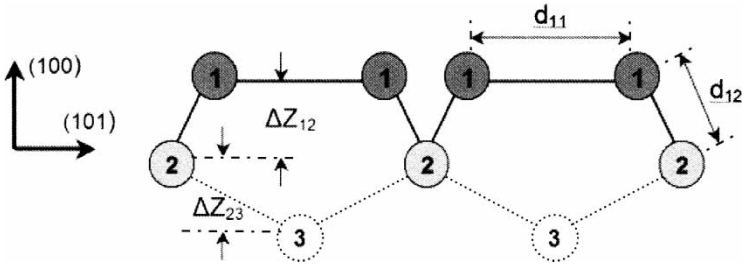

FIGURE 2 Schematic diagram of the ΔZ_{12} and ΔZ_{23} relaxations of the (100) (2 × 1) surface.

layer relaxation depths ΔZ_{12} and ΔZ_{23}, respectively (see Fig. 2). In the case of the (111) surface the reported features are the dimer lengths d_{11} and d_{12} for the (1 × 1) dimer, the (2 × 1) (π-bonded Pandey chain [21]) dimer (see Figs. 3 and 4) and the ($\sqrt{3} \times \sqrt{3}$) $R30^\circ$ surface trimer (see Fig. 5). In addition to this the bond angles α and β, as shown in Fig. 6, have also been considered for the (111) surface, both for the (2 × 1) and ($\sqrt{3} \times \sqrt{3}$) $R30^\circ$ reconstructions. The first and second layer relaxations have not been considered for the (111) surface, as the coexistence of more than one dimer pattern on the surface results in a complicated and variable surface relaxation.

Figure 7 gives the energy per atom as a function of MC iteration for the MC simulations of the (100) and (111) bulk diamond surfaces. The figure shows that the MC run had energy converged after approximately 150 million moves for the (111) surface and 175 million moves for the (100) surface. Figure 8 gives the convergence of the dimer lengths d_{11} and d_{12} as a function of MC iteration for the (100) surface and shows that structural convergence of the surface is closely aligned to its energy convergence. Therefore we believe the results obtained after 200 million MC moves are indicative of the equilibrium minimum energy configurations for the bulk diamond surfaces.

In addition we note that all of the dimers calculated in this study are comprised of only single bonds, which produces a residual single dangling bond per atomic site. While double bonds have a lower energy per surface dimer, single bonds have been reported by others [22] using empirical potentials. In general, double bonded dimers constitute a closed shell structure and are also characterised by shorter bond (d_{11}) lengths, while single bonds are biradical (and not a weak π-bond as often thought) with longer dimer lengths. Simulations of surface reconstruction using the empirical Brenner potential [7] does show that the dimer-bond in the (100) surface has the character of a double-bond which is also observed experimentally.

The Bulk Diamond (100) Surface

Monte-Carlo simulations of the diamond (100) surface were conducted by constructing a diamond slab of 10 × 10 × 7 unit cells, comprising 5600 atoms. Periodic boundary conditions were applied in the x and y directions, but were

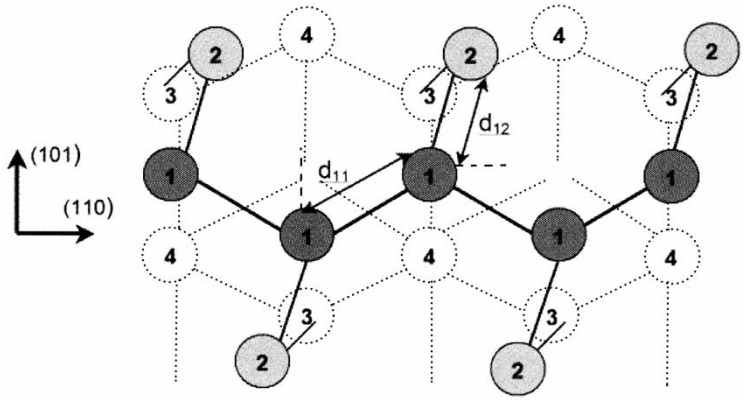

FIGURE 3 Schematic diagram of the d_{11} and d_{12} dimer lengths on the (111) (2 × 1) surface.

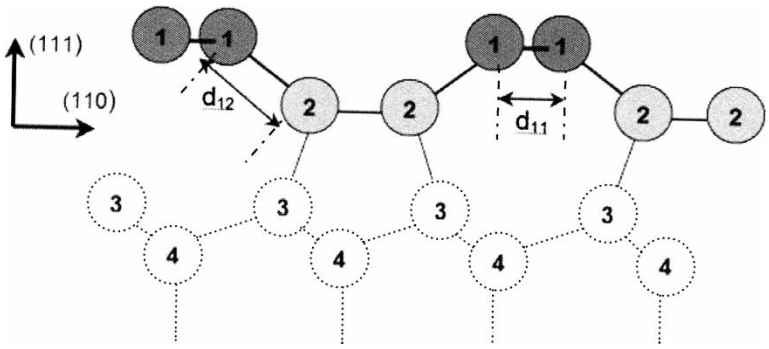

FIGURE 4 Schematic diagram of the d_{11} and d_{12} dimer lengths on the (111) (2 × 1) surface.

removed in the z direction thus producing two z surfaces giving a total surface area of approximately 713 Å^2. A vacuum space of 10 Å was added between the z surfaces and edges of the simulation super-cell. It has been found that effects of relaxation may be observed as deep as the 7th atomic layer [14]. So care was taken to ensure that the lattice was more than twice this depth in order to allow for full relaxation of the top and bottom surfaces. The results of the simulation are depicted in Fig. 9, showing the two upper most layers and the (2 × 1) reconstruction of the (100) surface, in accordance with the experimentally observed pattern (although the whole surface has not reconstructed). We believe that more extensive reconstruction would probably require longer runs on larger systems. Our calculations also show that once formed, dimer bonds are stable. For each MC run the (2 × 1) dimers were then characterized by considering the average interatomic distances d_{11} and d_{12}. Similarly the surface relaxation was measured by finding the average change in the atomic layer separations ΔZ_{12} and ΔZ_{23}. We may also see by inspection of Fig. 9 that the dimers are predominantly arranged in rows. This pattern has been found to be energetically favoured over a zigzag pattern, where dimers in respective positions interchange rows [13]. For the (100) surface, the values of the reconstruction parameters d_{11} and d_{12}, ΔZ_{12} and ΔZ_{23} averaged over all dimerisation events and simulated (100) surfaces in this study is given in Table I along with comparative theoretical and experimental results. The values of ΔZ_{12} and ΔZ_{23} in Table I corresponding to the interlayer spacing in the relaxed structure, it should be noted that recent *ab initio* calculations [4,14] do indicate that the clean C(100)(2 × 1) surface does from double bonded dimers: hence the shorter d_{11} dimer lengths shown in Table I, whereas our potential only predicts single bond dimerisation.

The Bulk Diamond (111) Surface

As the (111) surface proved to be more computationally intensive (due to the close packing of the (111) surface) a smaller system was used.

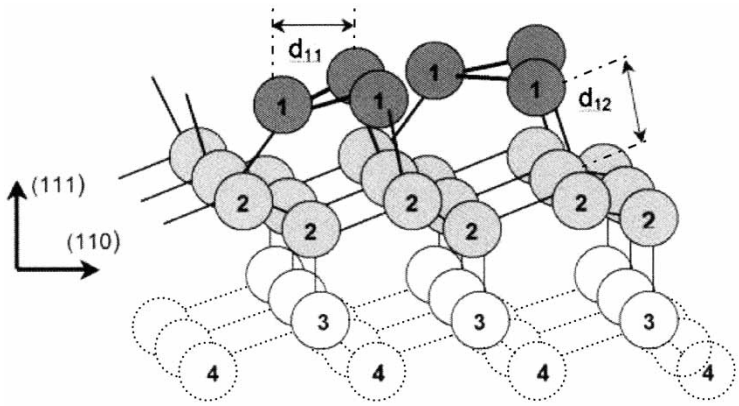

FIGURE 5 Schematic diagram of the d_{11} and d_{12} dimer lengths for the $(\sqrt{3}\times\sqrt{3})R30°$ surface trimer.

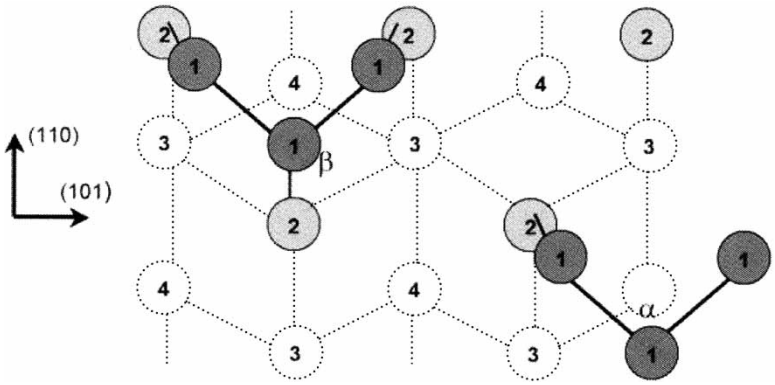

FIGURE 6 Schematic diagram of the α and β angles for the $(\sqrt{3}\times\sqrt{3})R30°$ (111) surface trimer.

Here a lattice of $4 \times 8 \times 6$ unit cells was constructed, comprising 2304 atoms. Periodic boundary conditions were applied in the y and z directions (giving a total surface area of approximately 342 Å^2), and removed in the x direction, where again a vacuum space of 10 Å was added. The MC simulation was once again run for 200 million moves and the results given in Table II. The reconstructed (111) surface exhibits a complicated mixture of dimer and trimer patterns, with the (1×1), (2×1) and the $(\sqrt{3}\times\sqrt{3})R30°$ reconstruction coexisting. The (2×1) Pandey chains are by far the most prevalent (seen as long and short jagged chains), followed by the (1×1) dimers and finally the $(\sqrt{3}\times\sqrt{3})R30°$ trimers. Figure 10 shows the first layer and second atomic layers on one (111) surface. While there are a number of instances of the (1×1) reconstruction, there is only one instance of the $(\sqrt{3}\times\sqrt{3})R30°$ reconstruction (seen in the lower left side of Fig. 10). Once again there are some unreconstructed sites which may have reconstructed by continuing the MC run for more moves or using a larger system.

The obtuse angle between any three consecutive atoms in a (2×1) chains and the three atoms comprising the $(\sqrt{3}\times\sqrt{3})R30°$ trimer have been denoted as α. This angle only involves atoms on the 1st atomic layer in both cases (being the angle between adjoining d_{11} dimers as shown in Fig. 6); however it may be located on "either-side" of the (2×1) chains.

In Fig. 11 the second atomic layer has been included so that the secondary dimer length d_{12} is apparent, along with the secondary angle β. The secondary dimers appear as an apparent "doubling" of the atoms shown in Fig. 10; but are better depicted by Fig. 1. The secondary angle β involves 2 atoms in the 1st atomic layer, and one in

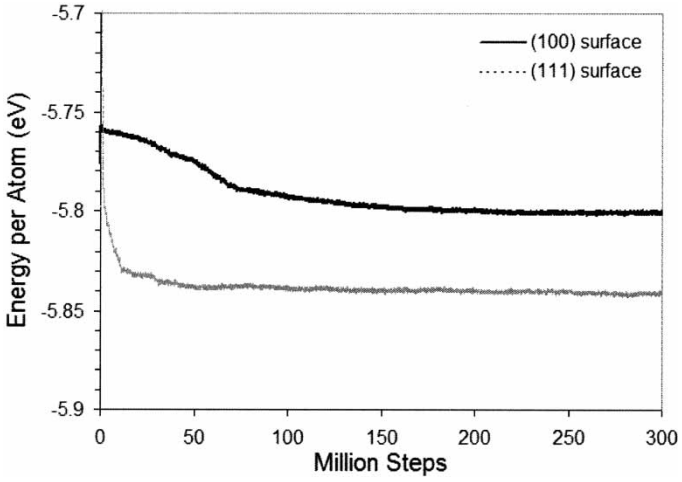

FIGURE 7 Energy convergence of the (100) and (111) surfaces up to 300 million moves.

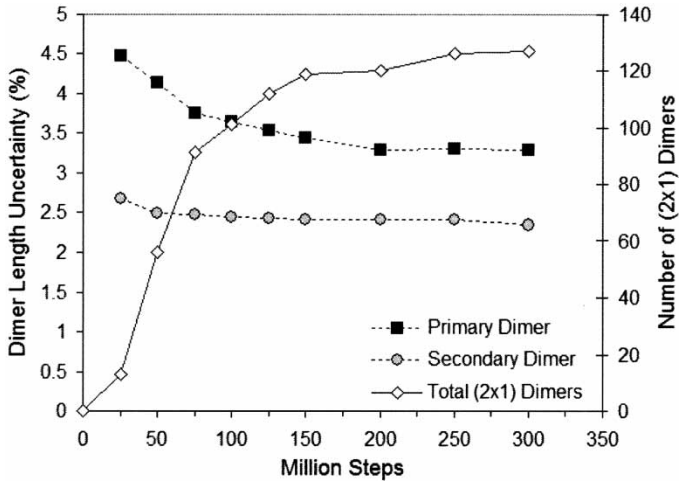

FIGURE 8 Structural convergence of the (100) surfaces up to 300 million moves.

the 2nd; hence β is the angle between adjoining d_{11} and d_{12} dimers (see Fig. 6).

Nanodiamond Crystals and Reconstruction

In this study, three nanodiamond crystal sizes were considered. These are listed in Table III, with the corresponding surface to volume ratio (ζ) and number of atoms in each crystals. The crystals were constructed using a using a Molecular CAD program, such that there are two (100) surface, and four (110) surfaces. As the (110) surface does not reconstruct and is considered stable the reconstruction of these crystals is entirely confined to the (100) surfaces, and may, therefore, be compared with the (100) surface reconstruction in "The bulk diamond (100) surface" section. The surface reconstruction of these nanodiamond structures was studied by performing MC runs, but with the periodic boundary conditions removed in all directions.

Each MC run was performed for 100 million moves 300 K, to ensure that the surfaces were close to their minimum energy configuration. Following reconstruction, the (100) surfaces were characterised with respect to d_{11} dimer length, d_{12} dimer length and compared to the bulk (100) surface results.

The effects of reconstruction in d_{11} and d_{12} for the nanodiamond crystals are contained within Table III, along with the corresponding values from bulk diamond. These results are also shown pictorially in Figs. 11 and 12. The 1/2 nm nanodiamond fully reconstructed, with a total of four d_{11} dimers forming (see Fig. 11). The 1 and 2 nm nanodiamonds had a total of 16 and 52 dimers, respectively, however while the 1 nm nanodiamond fully reconstructed with perfect row dimerisation (see Fig. 12), the 2 nm crystal exhibited row and zigzag d_{11} dimers, along

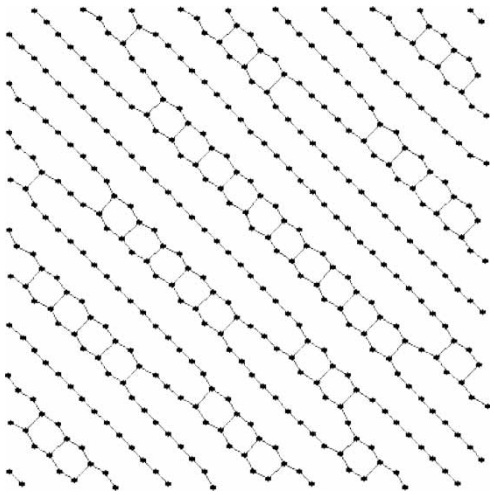

FIGURE 9 Reconstructed diamond (100) surface, showing only 1st (diagonal bars) and 2nd (adjoining chains) atomic layer.

TABLE I Surface reconstruction results for the (100) surface of diamond and comparative computational and experimental values

Parameter	This study	Original SW potential for diamond [23]	Comparative computational/ experimental results
d_{11} (Å)	1.68 ± 0.05	1.77 ± 0.06	1.542^{e}[6] 1.66^{e}[22] 1.58^{s}[24] 1.53^{s}[22] 1.40^{a}[4] 1.37^{a}[5]
d_{12}(Å)	1.56 ± 0.04	1.59 ± 0.04	1.515^{e}[6] 1.50^{s}[25]
ΔZ_{12}(Å)	0.86 ± 0.06 (−1.8%)	0.90 ± 0.05 (1.8%)	− 16.9%^{s}[24] 1.0^{ex}[25] 1.0 ± 0.1^{ex}[9]
ΔZ_{23}(Å)	0.97 ± 0.06 (+ 9.5%)	0.97 ± 0.08 (+ 10.1%)	+ 6.7%^{s}[24] + 3%^{a}[4]

Values are in units of Å. The symbols *e*, *s* and *a* refer to empirical, semi-*ab initio* and *ab initio* based calculations, respectively. The symbol *ex* refers to experimental results. The percentages give the percent change of the inter-layer spacing with respect to the bulk spacing.

TABLE II Surface reconstruction of the (111) surface of diamond and comparison with other computational results

Parameter	This study	Original SW potential for diamond [23]	Semi-*ab initio* [25]
$d_{11}(1\times1)$ (Å)	2.5 ± 0.5	2.13 ± 0.03	2.5
$d_{11}(2\times1)$ (Å)	1.59 ± 0.06	1.6 ± 0.15	1.39
$d_{12}(2\times1)$ (Å)	1.6 ± 0.13	1.7 ± 0.13	1.49
$\alpha(2\times1)$ (Deg)	103 ± 7.5	102 ± 4.7	121
$\beta(2\times1)$ (Deg)	102 ± 4.9	102 ± 5.1	114
$d_{11}(\sqrt{3}\times\sqrt{3})R30°$ (Å)	1.7 ± 0.13	1.64 ± 0.03	1.44
$d_{12}(\sqrt{3}\times\sqrt{3})R30°$ (Å)	1.62 ± 0.03	1.7 ± 0.14	1.56
$\alpha(\sqrt{3}\times\sqrt{3})R30°$ (Deg)	89 ± 7.4	97 ± 6.4	94
$\beta(\sqrt{3}\times\sqrt{3})R30°$ (Deg)	104 ± 1.2	103 ± 5.2	116

In the table above (1×1) d_{11} is an experimental LEED result as quoted in Ref. [25].

TABLE III Specifics of constructed nanodiamond crystals and surface results of the (100) nanodiamond

Property	$\frac{1}{2}$ nm	1 nm	2 nm	Bulk
Volume (nm^3)	0.16	1.29	9.61	–
$\zeta(nm^{-1})$	11.0	5.43	2.79	–
Number of Atoms	28	259	1798	–
d_{11} (Å)	1.60 ± 0.03	167 ± 0.03	1.68 ± 00.3	1.68 ± 0.05
d_{12} (Å)	1.58 ± 0.03	1.56 ± 0.03	1.57 ± 0.04	1.56 ± 0.04

ζ is the surface area to volume ratio.

with unreconstructed sites. Care was taken when constructing the crystals to ensure that each crystal was symmetric in all directions, and hence the opportunity existed for full and perfect reconstruction. The 1/2 nm and 1 nm crystals reconstructed perfectly (100% of possible dimers present), however, only 81% of possible dimer sites were occupied in the case of the 2 nm crystal. This is possibly because at the lower surface to volume ratio, a higher fraction of the accepted MC moves will involve bulk atoms, and a correspondingly lower fraction involve surface atoms. *ab initio* surface reconstruction calculations on the 259 atom C(100) nanodiamond [26,27] performed using the plane wave DFT package VASP [28] gave (2×1) reconstruction results comparable to those obtained using our potential. The *ab inito* calculations gave averaged reconstruction dimer lengths (d_{11} and d_{12}) of 1.44 ± 0.06 Å and 1.49 ± 0.08 Å, respectively. As shown in Table III the comparative SW results are 1.60 ± 0.03 Å and 1.58 ± 0.03 Å. Obviously system sizes of a few hundred atoms are within the range of *ab initio* or semi-*ab initio* investigation.

The aim of this study was to compare our results with those of obtained by more accurate methods to see if this potential could be used to obtain reasonably accurate results when applied to system sizes in the regime of 10^5 to 10^6 atoms. Further MC investigations of larger nanodiamond structures are continuing and will be reported at a later date.

CONCLUSION

The results of the diamond surface reconstruction were found to compare reasonably well with comparable results of other studies. In the case of the (100) surface of bulk diamond the d_{11} dimer length of 1.68 ± 0.05 Å (for a single bond) compare well with the results of other studies using empirical potentials. In general, simulations using empirical potentials such as SW were found to generate single bonded dimers, that have a longer d_{11} dimer length, than *ab initio* methods that yield a double bonded d_{11} dimer of length around 1.40 Å. The calculated value of 1.56 ± 0.04 Å for the d_{12} dimer length was found to compare very well with those results using a empirical Tersoff potential (1.515 Å) and with the value of 1.50 Å calculated by Frauenheim [25] using a semi-empirical approach. The calculation of the relaxation of the (100) surface also gave results within error of experiment. In the case of the (111) surface, the results show the (1×1) reconstruction is excellent agreement with the experimental value, however, the (2×1) results are significantly less then those of predicted by others [25].

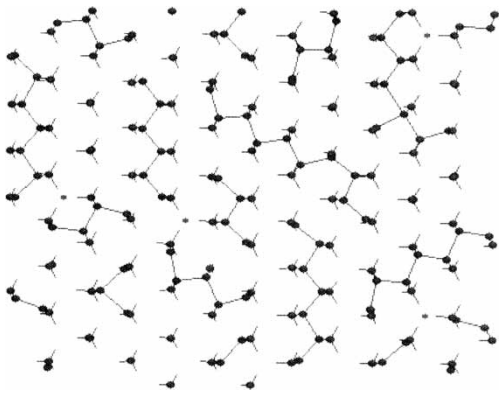

FIGURE 10 Reconstructed diamond surface, showing only 1st and 2nd atomic layers.

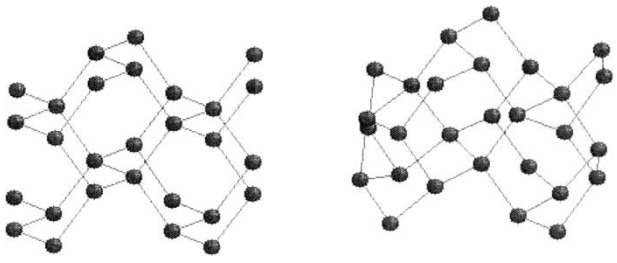

FIGURE 11 The 1/2 nm nanodiamond crystal before (left) and after (right) reconstruction.

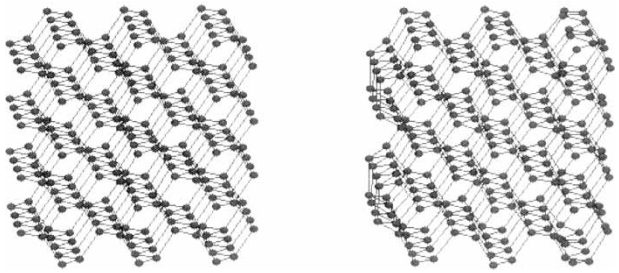

FIGURE 12 The 1 nm nanodiamond crystal before (left) and after (right) reconstruction.

Acknowledgements

The authors would like to thank the Victorian Partnership for Advanced Computing for support and access to their computing facilities and Mr Geoff Leach of Department of Computer Science, RMIT University, for supplying the molecular CAD program that was used in construction of the nanodiamond structures.

References

[1] Shkrebtii, A.I., Di Felice, R., Bertoni, C.M. and Del Sole, R. (1995) "*Ab initio* study of structure and dynamics of the Si(100) surface", *Phys. Rev. B* **51**, 11201.

[2] Takahashi, K., Nara, C., Yamagishi, T. and Onzawa, T. (1999) "Calculation of surface energy and simulation of reconstruction for Si(111) 3×3, 5×5, 7×7, and 9×9 DAS structure", *Surf. Sci.* **151**, 299.

[3] Weiner, B., Skokov, S. and Frenklach, M. (1995) "A theoretical analysis of a diamond (100)—(2×1) dimer bond", *J. Chem. Phys.* **102**(13), 5386.

[4] Yang, S.H., Drabold, D.A. and Adams, J.B. (1993) "*Ab initio* study of diamond C(100) surfaces", *Phys. Rev. B* **48**(8), 5261.

[5] Furthmüller, J., Hafner, J. and Kresse, G. (1996) "Dimer reconstruction and electronic surface states on clean and hydrogenated diamond (100) surfaces", *Phys. Rev. B* **48**, 7334.

[6] Petukhov, A.V., Fasolino, A., Passerone, D. and Ercolessi, F. (2000) "Reconstruction of Diamond (001) Surface: A Monte Carlo Study with the Tersoff Potential", *Phys. Stat. Sol. (a)* **174**, 19.

[7] Petukhov, A.V. and Fasolino, A. (2000) "Reconstructions of Diamond (100) and (111) Surfaces: Accuracy of the Brenner Potential", *Phys. Stat. Sol. (a)* **181**, 109.

[8] Dyson, A.J. and Smith, P.V. (1994) "Empirical molecular dynamics calculations for the (001) and (111) 2×1 reconstructed surfaces of diamond", *Surf. Sci.* **316**, 309.

[9] Stallcup, R.E. II, Aviles, A.F. and Perez, J.M. (1995) "Atomic resolution ultrahigh vacuum scanning tunneling microscopy of epitaxial diamond (100) films", *Appl. Phys. Lett.* **66**(18), 2331.

[10] Ravi, K.V., Oden, P.I. and Yaniv, D.R. (1993) In: Dismukes, J.P. and Ravi, K.V., eds, *Proceedings of the Third International Symposium on Diamond Materials* (Electrochemical Society, Pennington, NJ), p 766.

[11] Petukhov, A.V., Passerone, D., Ercolessi, F., Tosatti, E. and Fasolino, A. (2000) "Metastable reconstructions of the diamond (111) surface: Interplay between diamond and graphitelike bonding", *Phys Rev. B* **61**(16), 590.

[12] Jungnickel, G., Porezag, D., Frauenheim, TH., Lambrecht, W.R.L., Segall, B. and Angus, J.C. (1995) "Diamond (111) surface: graphitization or reconstruction?", *Mat. Res. Soc. Symp. Proc.* **338**, 349–360.

[13] Skokov, S., Weiner, B., Frenklach, M., Frauenheim, TH. and Sternberg, M. (1995) "Dimer-row pattern formation in diamond (100) growth", *Phys. Rev. B* **52**(7), 5426.

[14] Kern, G. (1998) "Clean and hydrogenated diamond and graphite surfaces", unpublished dissertation, Institut für Theoretische Physik, Technische Universität Wien.

[15] Barnard, A.S. and Russo, S.P. (2002) "Development of an Improved Stillinger–Weber potential for tetrahedral carbon using *ab-initio* (Hartree-Fock and MP2) methods", *Mol. Phys.* **100**(10), 1517–1525.

[16] Barnard, A.S., Russo, S.P. and Leach, G.I. (2002) "Nearest Neighbour Considerations in Stillinger–Weber type potentials for Diamond", *Mol. Sim.* **28**(8), 761–771.

[17] Drexler, K.E. (1992) *Nanosystems, Molecular Machinery, Manufacturing and Computation* (Wiley, New York).

[18] Gould, H. and Tobochnik, J. (1996) *An introduction to computer simulation methods: application to physical systems*, 2nd Ed. (Addision-Wesley).

[19] Stillinger, F.H. and Weber, T.A. (1985) "Computer simulation of local order in condensed phases of silicon", *Phys. Rev. B* **31**, 5262.

[20] Lurie, P.G. and Wilson, J.M. (1977) "The diamond surface: I. The structure of the clean surface and the interaction with gases and metals", *Surf. Sci.* **65**, 453.

[21] Pandey, K.C. (1981) "New *pi*-Bonded Chain Model for Si(111)—(2×1) Surface", *Phys. Rev. Lett.* **47**, 1913.

[22] Skokov, S., Carmer, C.S., Weiner, B. and Frenklach, M. (1994) "Reconstruction of (100) diamond surfaces using molecular dynamics with combined quantum and empirical forces", *Phys. Rev. B* **49**(8), 5662.

[23] Pailthorpe, B.A. (1991) "Molecular-dynamics simulations of atomic processes at the low-temperature diamond (111) surface", *J. App. Phys.* **70**, 543.

[24] Mehandru, S.P. and Anderson, A.B. (1991) "Adsorption of H, CH_3, CH_2 and C_2H_2 on 2×1 restructured diamond (100): Theoretical study of structures, bonding, and migration", *Surf. Sci.* **248**, 369.

[25] Frauengeim, T.H., Stephan, U., Blaudeck, P., Porezag, D., Busmann, H.-G., Zimmerman-Edling, W. and Lauer, S. (1993) "Stability, reconstruction, and electronic properties of diamond (100) and (111) surfaces", *Phys. Rev. B* **48**(24), 18189.

[26] Barnard, A.S., Russo, S.P. and Snook, I.K. (2003) "*Ab initio* modelling of the stability of nanocrystalline diamond morphologies", *Phil. Mag. Lett.* **83**(1), 39–45.

[27] Russo, S.P., Barnard, A.S. and Snook, I.K. (2003) "Hydrogenation of Nanodiamond Surfaces: Structure and Effects on Crystalline Stability", *Surf. Rev. Lett.* **10**(2), 233.

[28] Kresse, G. and Hafner, J. (1996) "Efficient iterative schemes for *ab initio* total-energy calculations using a plane-wave basis set", *Phys. Rev. B* **54**, 11169.